BIOCHEMISTRY
including biophysical chemistry & molecular biology

ARTICLE

pubs.acs.org/biochemistry

Ground-State Destabilization in Orotate Phosphoribosyltransferases by Binding Isotope Effects

Yong Zhang and Vern L. Schramm*

Department of Biochemistry, Albert Einstein College of Medicine, Bronx, New York 10461, United States

Supporting Information

ABSTRACT: Orotate phosphoribosyltransferases (OPRTs) form and break the *N*-ribosidic bond to pyrimidines by way of ribocation-like transition states (TSs) and therefore exhibit large α-secondary 1′-^{3}H k_{cat}/K_m kinetic isotope effects (KIEs) [Zhang, Y., and Schramm, V. L. (2010) *J. Am. Chem. Soc. 132*, 8787−8794]. Substrate binding isotope effects (BIEs) with OPRTs report on the degree of ground-state destabilization for these complexes and permit resolution of binding and transition-state effects from the k_{cat}/K_m KIEs. The BIEs for interactions of [1′-^{3}H]orotidine 5′-monophosphate (OMP) with the catalytic sites of *Plasmodium falciparum* and human OPRTs are 1.104 and 1.108, respectively. These large BIEs establish altered sp^3 bond hybridization of C1′ toward the sp^2 geometry of the transition states upon OMP binding. Thus, the complexes of these OPRTs distort OMP part of the way toward the transition state. As the [1′-^{3}H]OMP k_{cat}/K_m KIEs are approximately 1.20, half of the intrinsic k_{cat}/K_m KIEs originate from BIEs. Orotidine, a slow substrate for these enzymes, binds to the catalytic site with no significant [1′-^{3}H]orotidine BIEs. Thus, OPRTs are unable to initiate ground-state destabilization of orotidine by altered C1′ hybridization because of the missing 5′-phosphate. However the k_{cat}/K_m KIEs for [1′-^{3}H]orotidine are also approximately 1.20. The C1′ distortion for OMP happens in two steps, half upon binding and half on going from the Michaelis complex to the TS. With orotidine as the substrate, there is no ground-state destabilization in the Michaelis complexes, but the C1′ distortion at the TS is equal to that of OMP. The large single barrier for TS formation with orotidine slows the rate of barrier crossing.

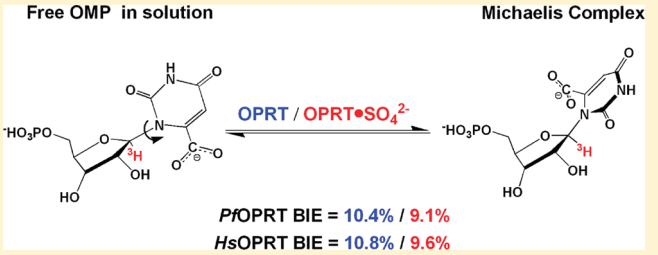

Intrinsic kinetic isotope effects (KIEs) are commonly used to provide bond structural information for enzymatic transition states (TSs). Competing isotopic label methods provide KIEs on the k_{cat}/K_m kinetic parameter,[1,2] but the k_{cat}/K_m KIEs include all kinetically important steps between reactants free in solution and the first irreversible step of the reaction (Figure 1).[3] Via measurement of equilibrium binding isotope effects (BIEs), bond vibrational changes upon formation of the Michaelis complex are obtained and KIEs from the chemical step can be resolved.[4] Reactions involving *N*-ribosidic bond loss commonly form ribocation transition states in which the anomeric carbon undergoes rehybridization from sp^3 in the reactant to sp^2 at the transition state. α-Secondary 1′-^{3}H BIEs are a sensitive way of measuring bonding changes in reactants upon binding to catalytic sites and therefore report on the degree of ground-state destabilization for the enzyme−substrate complexes. Enzyme-based ground-state destabilization is established for several enzymes and has been summarized by Anderson,[5] although earlier reports have questioned the ability of enzymes to distort substrates.[6]

Recent BIE studies with purine nucleoside phosphorylase (PNP) reported a 5′-^{3}H BIE remote from the site of chemical bond breaking and gave a BIE of 1.5%. For TS analogues of PNP, normal 5′-^{3}H BIEs of 13−29% were reported for human PNP, indicating that TS analogue interactions differ considerably from those in Michaelis complexes or at the TS.[7] BIEs with PNP were explained by local C5′−H5′ bond distortion and are not necessarily linked to ground-state destabilization. Ground-state destabilization can be established by BIEs of atoms involved in the chemical reaction by showing that the distortion leads toward the transition state.

Orotate phosphoribosyltransferases from *Plasmodium falciparum* (*Pf*OPRT) and human sources (*Hs*OPRT) catalyze the reversible pyrophosphorolysis of orotidine and orotidine 5′-monophosphate (OMP). Transition-state analyses using isotope effects and quantum chemical calculations have established ribocation TS structures with fully dissociated dianionic orotates (Figure 1).[8,9] Large normal α-secondary 1′-^{3}H k_{cat}/K_m intrinsic KIEs of 19−26% were measured for reactions catalyzed by *Pf*OPRT and *Hs*OPRT. These isotope effects are primarily the result of out-of-plane bending mode changes as the C1′ geometry is distorted from sp^3 in the reactant to sp^2 at the S_N1 TS. Secondary 1′-^{3}H k_{cat}/K_m KIEs from in vacuo calculations provide a two-state model for the conversion of unbound reactants to the transition state. In reality, k_{cat}/K_m KIEs also include changes to the 1′-^{3}H bond vibrational changes in the Michaelis complex. Here we use BIE to resolve these effects.

The X-ray crystal structure of *Hs*OPRT in complex with OMP [Protein Data Bank (PDB) entry 2WNS] proposes multiple

Received: April 26, 2011
Published: April 28, 2011

 © 2011 American Chemical Society

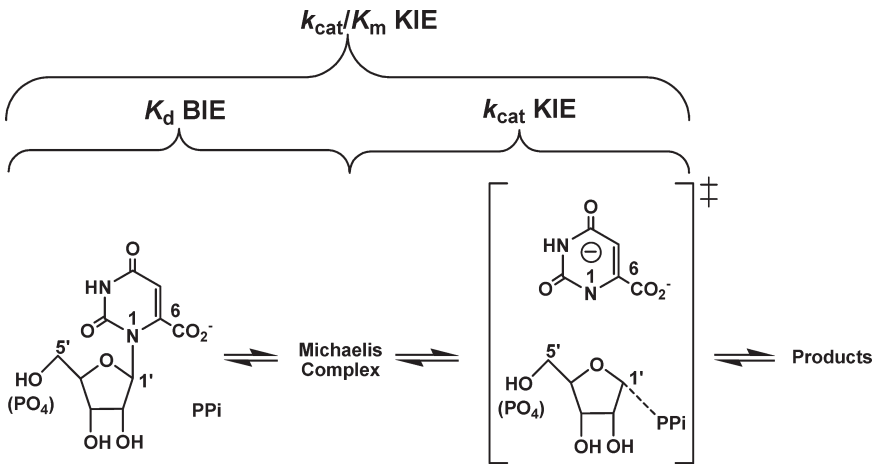

Figure 1. Reaction catalyzed by *Plasmodium falciparum* OPRT and *Homo sapien* OPRT and the relationship among BIE, k_{cat}/K_m KIE, and k_{cat} KIE. The substrate pair of orotidine and pyrophosphate (PP_i) is shown. A similar transition state is formed when PP_i is replaced with phosphonoacetic acid. Transition-state features are shown in brackets.

catalytic site contacts to OMP. Structural models predict an extended hydrogen bond network surrounding the pyrimidine group to enforce leaving group activation. Leaving group forces have been confirmed in OPRT by isotope-edited Fourier transform infrared (FTIR) spectroscopy of the pyrimidine group.[10] Enzyme-bound OMP differs in geometry from the in vacuo energy minimum, most obviously for the *N*-ribosyl torsion angle between the orotate base and ribose ring. The 1′-^{3}H bond vibrations are sensitive to the *N*-ribosyl torsion angle.[11] When the enzyme stabilizes a conformation away from the energetic minimum of the unbound substrate, the degree of sp^3 hybridization at C1′ may be altered to cause a BIE.[12]

Here, 1′-^{3}H BIEs of OMP and orotidine were measured in binary and ternary complexes of *Pf*OPRT and *Hs*OPRT. Large normal BIEs with [1′-^{3}H]OMP (alone or with sulfate, a competitive inhibitor with pyrophosphate) demonstrate ground-state destabilization toward the TS. The lack of [1′-^{3}H]orotidine BIEs indicates that without the 5′-phosphate, the substrate undergoes no significant distortion in the Michaelis complexes. This is the first work to report a 1′-^{3}H BIE for any *N*-ribosyltransferase. In combination with experimental KIEs, the 1′-^{3}H BIEs reveal the 5′-phosphate to assist in a two-step C1′ distortion for OPRT-catalyzed OMP pyrophosphorolysis.

MATERIALS AND METHODS

Reagents. D-[1-^{3}H]Ribose and D-[6-^{14}C]glucose were purchased from American Radiolabeled Chemicals Inc. Hexokinase (HK), glucose-6-phosphate dehydrogenase (G6PDH), phosphogluconic acid dehydrogenase (PGDH), L-glutamic acid dehydrogenase (GDH), phosphoriboisomerase (PRI), adenylate kinase (AK), and pyruvate kinase (PK) were purchased from Sigma-Aldrich. Phospho-D-ribosyl-α-1-pyrophosphate synthase (PRPPase) and ribokinase (RK) were prepared as described previously.[13,14] Alkaline phosphatase (AP) was purchased from Roche Applied Science. *Pf*OPRT and *Hs*OPRT were expressed in *Escherichia coli* cells and purified as described previously.[8] All other reagents were purchased from readily available commercial sources and used without further purification.

Synthesis of Isotopically Labeled OMPs and Orotidines. Isotopically labeled OMPs were synthesized enzymatically as previously described.[8] Orotidines were prepared from OMPs on the basis of a previous report.[9]

Quantum Chemical Calculations. The OMP structures were calculated in vacuo using hybrid density functional theory implemented in Gaussian 03.[15] The initial model of OMP bound to *Hs*OPRT was from the crystal structure of *Hs*OPRT in complex with OMP (PDB entry 2WNS). At the B3LYP/6-31G(d,p) level, geometry optimizations were performed for *Hs*OPRT-bound OMP with dihedral angles fixed to those in the crystal structure and free OMPs with restricted O4′−C1′−N1−C2 dihedral angles. Bond frequencies of the optimized OMPs were calculated at the same level of theory and basis set. BIEs were calculated from the computed frequencies of free OMPs and *Hs*OPRT-bound OMP at 298 K using ISOEFF98.[16]

Determination of Binding Isotope Effects. Competitive binding of [1′-^{3}H]OMP and [5′-^{14}C]OMP and competitive binding of [1′-^{3}H]orotidine and [5′-^{14}C]orotidine were measured with and without sulfate, using the ultrafiltration method.[12,17] Sulfate binds competitively to pyrophosphate (PP_i) binding sites of *Pf*OPRT and *Hs*OPRT and is chemically inert. With OMP as a substrate, the K_i of sulfate is 3.1 ± 0.3 mM for *Pf*OPRT and 17.6 ± 2.8 mM for *Hs*OPRT. With orotidine as a substrate, sulfate has a K_i of 2.7 ± 0.3 mM for *Pf*OPRT and 10.8 ± 1.6 mM for *Hs*OPRT. Measurements of 1′-^{3}H BIEs in binary complexes were taken in 50 mM Tris-HCl (pH 8.0), 20−500 μM OMP or orotidine (^{3}H:^{14}C ratio of disintegrations per minute: 4:1), and 10−300 μM *Pf*OPRT or *Hs*OPRT in a final volume of 100 μL. Measurements of 1′-^{3}H BIEs in ternary complexes included, in addition, 30−200 mM sulfate ($11K_i$) and 1 molar equiv of magnesium in a volume of 100 μL. Samples were loaded into the upper well of the ultrafiltration apparatus, and 30 psi of argon pressure was applied until approximately half of the solution had passed through the dialysis membrane (12−14 kDa molecular mass cutoff) into the lower well (60−90 min). Samples (30 μL) from the upper and lower wells were mixed with 10 mL of scintillation fluid (Ultima Gold) and counted for at least six cycles (10 min per cycle). Spectral deconvolution of ^{3}H and ^{14}C was performed using a ^{14}C standard in a matrix identical to that of the BIE samples. The BIE was calculated from eq 1

$$\mathrm{BIE} = \frac{{}^{14}C_T/{}^{14}C_B - 1}{{}^{3}H_T/{}^{3}H_B - 1} \quad (1)$$

dx.doi.org/10.1021/bi200638x |*Biochemistry* 2011, 50, 4813–4818

Table 1. 1′-^{3}H BIEs and k_{cat}/K_m KIEs for *Pf*OPRT and *Hs*OPRT

		[1′-^{3}H]OMP vs [5′-^{14}C]OMP	
		OPRT·OMP binary complex	OPRT·OMP·SO_4^{2-} ternary complex
BIE[a]	*Pf*OPRT	1.104 ± 0.002	1.091 ± 0.003
	*Hs*OPRT	1.108 ± 0.003	1.096 ± 0.004
K_d (μM)	*Pf*OPRT	3.1 ± 1.6	5.6 ± 1.8
	*Hs*OPRT	2.5 ± 1.2	4.1 ± 2.5
KIE[b]	*Pf*OPRT	1.261 ± 0.014 (exptl)	1.335 (calcd)
	*Hs*OPRT	1.199 ± 0.015 (exptl)	1.330 (calcd)
K_m[b] (μM)	*Pf*OPRT	3.7 ± 1.4	
	*Hs*OPRT	1.6 ± 0.6	
		[1′-^{3}H]orotidine vs [5′-^{14}C]orotidine	
		OPRT·orotidine binary complex	OPRT·orotidine·SO_4^{2-} ternary complex
BIE[a]	*Pf*OPRT	0.997 ± 0.003	0.991 ± 0.006
	*Hs*OPRT	0.999 ± 0.003	0.991 ± 0.005
K_d (μM)	*Pf*OPRT	130 ± 34	160 ± 30
	*Hs*OPRT	140 ± 27	150 ± 22
KIE[b]	*Pf*OPRT	1.189 ± 0.006 (exptl)	1.405 (calcd)
	*Hs*OPRT	1.209 ± 0.004 (exptl)	1.411 (calcd)
K_m[b] (μM)	*Pf*OPRT	96 ± 40	
	*Hs*OPRT	91 ± 37	

[a] BIE ± standard error. Each BIE was measured with at least four replicates. [b] From refs 8 and 9.

where $^{14}C_T$ and $^{14}C_B$ are the ^{14}C counts in the top and bottom wells, respectively, and ^3H_T and ^3H_B are the ^{3}H counts in the top and bottom wells, respectively.[7]

RESULTS AND DISCUSSION

1′-^{3}H BIEs of OMP and Orotidine. Upon formation of the binary complexes, [1′-^{3}H]OMP generates a BIE of 1.104 for *Pf*OPRT and a BIE of 1.108 for *Hs*OPRT (Table 1). The large normal BIEs indicate that C1′−H1′ bonds become less constrained in the Michaelis complexes relative to those of free OMPs in solution. α-Secondary 1′-^{3}H BIEs are dominated by out-of-plane bending modes, and these isotope effects establish sp^3 distortion at C1′, toward the sp^2 geometry of the transition state. The result is an unequivocal demonstration of reactant ground-state destabilization by enzymatic interactions. Comparison of [1′-^{3}H]OMP BIEs and KIEs reveals that C1′ distortion for OMP occurs in two steps, half upon binding and half upon going from the Michaelis complex to the TS.

In contrast to OMP, [1′-^{3}H]orotidine in the binary complexes shows BIEs of 0.997 and 0.999 for *Pf*OPRT and *Hs*OPRT, respectively (Table 1). The near-unity 1′-^{3}H BIEs for orotidine reflect no significant C1′ distortion upon binding to the OPRT active sites. Although the 5′-phosphate of OMP is remote from the reaction center, it is essential in anchoring the orotidine group to permit ground-state destabilization at the anomeric carbon. Without the 5′-phosphate group, orotidine is docked into the active site without significant C1′ ground-state destabilization, but the C1′ distortion at the TS is equal to that of OMP because k_{cat}/K_m KIE values are similar. Relative to OMP, orotidine has a 25-fold higher K_m and a 240-fold lower k_{cat}/K_m for both OPRT enzymes. The single large barrier for TS formation with orotidine as the substrate slows the rate of barrier crossing. The [1′-^{3}H]orotidine BIEs demonstrate the importance of the 5′-phosphate group for ground-state destabilization in the OPRT complexes. Altered kinetic properties have been reported for other enzymes with phosphate groups remote from the site of chemistry.[18−21] Here, BIEs demonstrate that the remote phosphate binding effect is required for anomeric carbon distortion toward the TS.

In the presence of sulfate, the ternary complexes give [1′-^{3}H]OMP BIEs of 1.091 for *Pf*OPRT and 1.096 for *Hs*OPRT. In contrast, [1′-^{3}H]orotidine BIEs are 0.991 for both enzymes (Table 1). Compared to BIEs determined for the binary complexes, 1′-^{3}H BIEs from the ternary complexes decrease ∼1%. Decreased 1′-^{3}H BIEs correspond to small conformational constraints in the C1′−H1′ bonds to demonstrate that bound sulfate causes a small constraint to the H1′ out-of-plane modes.

Dissociation Constants. The ultrafiltration method used for BIE experiments also permits measurement of dissociation constants of OMP and orotidine in the binary and ternary complexes. For *Pf*OPRT, the K_d values of OMP with and without sulfate are 5.6 and 3.1 μM, respectively, similar to its K_m value of 3.7 μM (Table 1). Orotidine has K_d values of 160 and 130 μM for *Pf*OPRT with and without sulfate, respectively, similar to its K_m of 96 μM with pyrophosphate. In the *Hs*OPRT ternary complexes, K_d values of OMP and orotidine are 4.1 and 150 μM, respectively. For the binary complexes, the K_d values are 2.5 and 140 μM for OMP and orotidine, respectively, similar to their corresponding K_m values of 1.6 and 91 μM with pyrophosphate, respectively. The similarity of dissociation constants with sulfate compared to the K_m values for OMP and orotidine with pyrophosphate supports similar interactions at the catalytic sites. These values are consistent with the transition-state structures of the OPRTs in which only weak van der Waals interactions are

dx.doi.org/10.1021/bi200638x |*Biochemistry* 2011, 50, 4813–4818

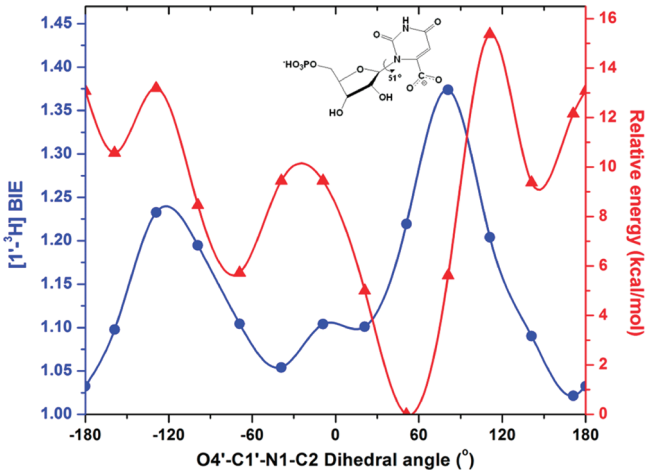

Figure 2. Calculated effects (in vacuo) of rotating the O4′−C1′−N1−C2 dihedral angle of free OMP on its relative energy (red). The calculated distortional [1′-^{3}H]OMP BIE (blue) compares different OMP solution-state geometries to the OPRT crystallographic torsion angle for bound OMP of 167°. The distortional BIEs were calculated using ISOEFF98.[16] The energy-minimized OMP with an O4′−C1′−N1−C2 dihedral angle of 51° is shown. Note the BIE is at a minimum at 167° (free and bound substrate at 167°). For a solution structure of 51°, distorted to 167°, the geometry found on the enzyme, the predicted distortional BIE is 1.22.

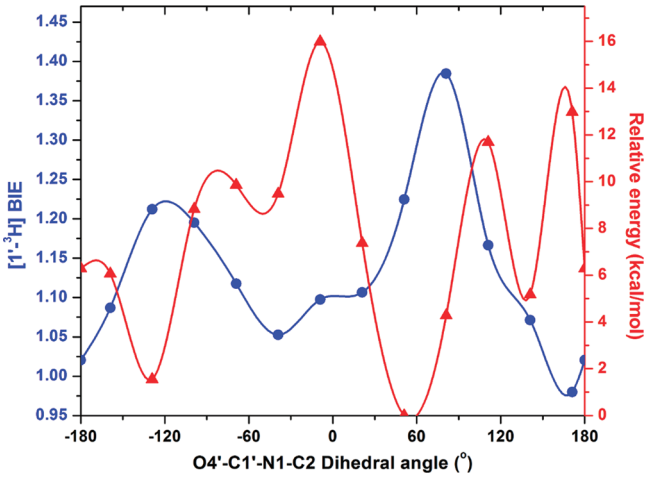

Figure 3. Calculated effects (in water) of rotating the O4′−C1′−N1−C2 dihedral angle of free OMP on its relative energy (red). The calculated distortional [1′-^{3}H]OMP BIE (blue) compares different OMP solution-state geometries to the OPRT crystallographic torsion angle for bound OMP of 167°. Using free OMPs with varied O4′−C1′−N1−C2 dihedral angles and *Hs*OPRT-bound OMP at 167°, theoretical BIEs were calculated using ISOEFF98. Calculations in water were performed using the Onsager model implemented in Gaussian 03. The recommended radii for calculations in water were determined via volume calculations.

present for the attacking nucleophile until the TS has been reached.[8,9]

Origin of the 1′-^{3}H BIE. Large normal 1′-^{3}H BIEs reflect bonding changes at the anomeric carbon upon formation of the Michaelis complexes. As the geometry of the O4′−C1′−N1−C2 dihedral angle changes from the energetic minimum of 51° for free OMP in vacuo to the specific value of 167° for OMP bound to *Hs*OPRT (PDB entry 2WNS), the change in C1′ hybridization results in a predicted 1′-^{3}H isotope effect (Figure 2). When the torsion angle changes from 51° to 167°, isotope effects of approximately 1.20 are predicted in vacuo and in water (Figures 2 and 3). Although 1′-^{3}H isotope effects are notorious in their difficulty to match computationally,[22] the calculations predict BIEs in the correct direction and toward the TS and demonstrate relatively small changes in C1′−H1′ bond length (1.092 and 1.094 Å). However, the C2′−C1′−H1′ bond angles reveal significant sp^3 distortion, changing from 108.7° and 113.6°, a change in C1′ hybridization from sp$^{2.7}$ to sp$^{2.47}$ (NBO analysis). These stereoelectronic changes establish OMP ground-state destabilization toward the sp^2 TSs of the OPRTs.

The [1′-^{3}H]OMP BIEs in Figures 2 and 3 are calculated purely on the *N*-ribosyl torsion angle and associated structural changes and overestimate the experimental BIEs in vacuo and in water. Clearly, the enzymes contribute additional changes that are known to influence the C1′−^{3}H1′ bond.[23−27] Upon formation of the Michaelis complex, distorted OMP displays a C4′−O4′−C1′−N1 dihedral angle of −118°, compared with a value of −151° calculated for free OMP.

The strained OMP causes orbital overlap between a lone pair of O4′ and the antibonding orbital (σ^*) of the C1′−N1 bond, promoting *N*-glycosidic bond cleavage. Ground-state distortion of OMP at the OPRT binding site is assisted by this effect. The antibonding orbital (σ^*) of the C1′−H1′ bond is antiperiplanar to a lone pair of O4′. The orbital interactions combined with an anomeric effect collectively contribute to the 1′-^{3}H BIEs.

Computational Analysis of the [1′-^{3}H]OMP BIE. X-ray crystal structures of OPRT homologues reveal large conformational changes involving catalytic site loop motions upon binding of substrates or products.[28−31] These motions form contacts to catalytic site reactants and are components of the reaction coordinate.[32−36] One mechanism for generating [1′-^{3}H]OMP BIEs is to immobilize the pyrimidine and ribosyl groups in different positions on the enzyme relative to those free in solution. Comparison of free and enzyme-bound dihedral angles gives a calculated [1′-^{3}H]OMP BIE of 1.219, greater than the experimental [1′-^{3}H]OMP BIE of 1.108, indicating that forces other than the *N*-ribosidic torsion angle contribute to the BIE. As required by this analysis, the calculated BIE values are unity at 167°, comparing like states on and off the enzyme.

Differences in calculated and experimental BIEs could be due to the anionic 6-carboxyl group of OMP (Figure 2). In vacuo calculations can overestimate intramolecular interactions between the 6-carboxylate anion and the 2′-hydroxyl group.

Calculation of the reactant state of OMP in water also overestimates the 1′-^{3}H BIE to be 1.225 (Figure 3). Calculated dihedral torsion angle energy barriers in water are decreased substantially but still give large 1′-^{3}H BIE values (Figure 4).

The calculations described above used the energetic minimum as a fixed value for calculation, and free-energy-weighted averages of [1′-^{3}H]OMP BIEs were calculated to be 1.216 in vacuo and 1.223 in water, close to those values determined from free OMP geometries as global minima.

[1′-^{3}H]OMP BIEs and KIEs for *Hs*OPRT. Resolution of the [1′-^{3}H]OMP k_{cat}/K_m KIE into binding and transition-state effects shows that half of the k_{cat}/K_m KIE originates from BIE and establishes two-step distortion of OMP at the OPRT active sites, half upon binding and half on going from the Michaelis

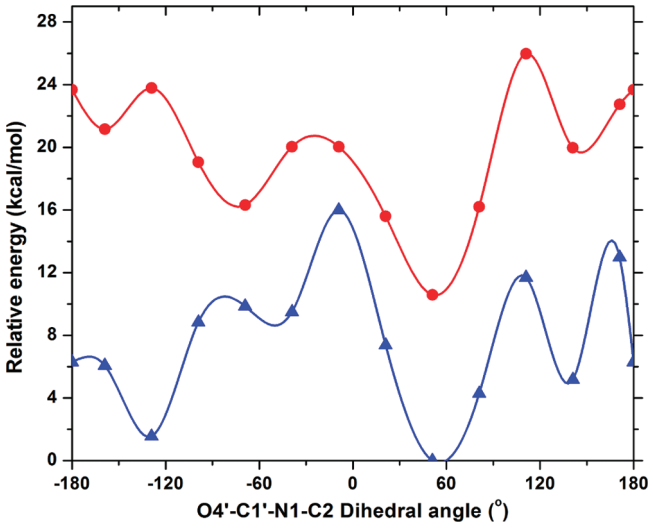

Figure 4. Effects of rotating the O4′−C1′−N1−C2 dihedral angle in OMP on the relative energy for free OMP calculated in vacuo (red) and in water (blue). Calculations in water were performed using the Onsager model implemented in Gaussian 03. The recommended radii for calculations in water were determined via volume calculations.

complex to the TS. In comparison, the near-unity [1′-^{3}H]orotidine BIE for *Hs*OPRT indicates that the experimental k_{cat}/K_m KIE of 1.209 has no contribution from the binding step and there is no significant ground-state destabilization in the Michaelis complexes.

CONCLUSION

These are the first reports of 1′-^{3}H BIEs in any *N*-ribosyltransferases. The large normal [1′-^{3}H]OMP BIEs reveal significant ground-state destabilization upon formation of the Michaelis complexes of *Pf*OPRT and *Hs*OPRT. The result is an unequivocal demonstration of substrate distortion toward the transition state. Half of the [1′-^{3}H]OMP KIE found at the sp^2 TS for these enzymes originates upon formation of the enzyme−substrate complexes. The ability of the OPRT enzymes to distort the sp^3 geometry of C1′ requires that the substrate be anchored by the 5′-phosphate. Orotidine passes through the same sp^2 TS but without ground-state destabilization and a 240-fold penalty in catalytic efficiency. Distortion of the geometry of C1′ is also known to occur upon binding of a transition-state analogue to human PNP.[37] Here we demonstrate that similar changes can occur upon substrate binding. 1′-^{3}H BIEs for OMP and orotidine with and without sulfate provide unique and valuable insights into interactions within the enzyme−substrate complexes.

ASSOCIATED CONTENT

Supporting Information. Complete calculation results. This material is available free of charge via the Internet at http://pubs.acs.org.

AUTHOR INFORMATION

Corresponding Author

*Department of Biochemistry, Albert Einstein College of Medicine, 1300 Morris Park Ave., Bronx, NY 10461. Phone: (718) 430-2813. Fax: (718) 430-8565. E-mail: vern.schramm@einstein.yu.edu.

Funding Sources

This work was supported by grants from the National Institutes of Health (AI049512 and GM041916).

ABBREVIATIONS

BIEs, binding isotope effects; OMP, orotidine 5′-monophosphate; *Pf*OPRT, *P. falciparum* orotate phosphoribosyltransferase; *Hs*OPRT, human orotate phosphoribosyltransferase; KIEs, kinetic isotope effects; TS, transition state; PNP, purine nucleoside phosphorylase; PP_i, pyrophosphate; FTIR, Fourier transform infrared.

REFERENCES

(1) Cleland, W. W. (1982) The use of isotope effects to determine transition-state structure for enzymic reactions. *Methods Enzymol. 87*, 625–641.

(2) Northrop, D. B. (1981) The expression of isotope effects on enzyme-catalyzed reactions. *Annu. Rev. Biochem. 50*, 103–131.

(3) Schramm, V. L. (2005) Enzymatic transition states: Thermodynamics, dynamics and analogue design. *Arch. Biochem. Biophys. 433*, 13–26.

(4) Schramm, V. L. (2007) Binding isotope effects: Boon and bane. *Curr. Opin. Chem. Biol. 11*, 529–536.

(5) Anderson, V. E. (2005) Quantifying energetic contributions to ground state destabilization. *Arch. Biochem. Biophys. 433*, 27–33.

(6) Fersht, A. (1999) in *Structure and mechanism in protein science: A guide to enzyme catalysis and protein folding*, p 373, W. H. Freeman, New York.

(7) Murkin, A. S., Tyler, P. C., and Schramm, V. L. (2008) Transition-state interactions revealed in purine nucleoside phosphorylase by binding isotope effects. *J. Am. Chem. Soc. 130*, 2166–2167.

(8) Zhang, Y., Luo, M., and Schramm, V. L. (2009) Transition states of *Plasmodium falciparum* and human orotate phosphoribosyltransferases. *J. Am. Chem. Soc. 131*, 4685–4694.

(9) Zhang, Y., and Schramm, V. L. (2010) Pyrophosphate interactions at the transition states of *Plasmodium falciparum* and human orotate phosphoribosyltransferases. *J. Am. Chem. Soc. 132*, 8787–8794.

(10) Zhang, Y., Deng, H., and Schramm, V. L. (2010) Leaving group activation and pyrophosphate ionic state at the catalytic site of *Plasmodium falciparum* orotate phosphoribosyltransferase. *J. Am. Chem. Soc. 132*, 17023–17031.

(11) Cocinero, E. J., Carcabal, P., Vaden, T. D., Simons, J. P., and Davis, B. G. (2011) Sensing the anomeric effect in a solvent-free environment. *Nature 469*, 76–79.

(12) Lewis, B. E., and Schramm, V. L. (2003) Binding equilibrium isotope effects for glucose at the catalytic domain of human brain hexokinase. *J. Am. Chem. Soc. 125*, 4785–4798.

(13) Parkin, D. W., Leung, H. B., and Schramm, V. L. (1984) Synthesis of nucleotides with specific radiolabels in ribose. Primary ^{14}C and secondary ^{3}H kinetic isotope effects on acid-catalyzed glycosidic bond hydrolysis of AMP, dAMP, and inosine. *J. Biol. Chem. 259*, 9411–9417.

(14) Singh, V., Lee, J. E., Nunez, S., Howell, P. L., and Schramm, V. L. (2005) Transition state structure of 5′-methylthioadenosine/S-adenosylhomocysteine nucleosidase from *Escherichia coli* and its similarity to transition state analogues. *Biochemistry 44*, 11647–11659.

(15) Frisch, M. J., (2004) *Gaussian 03*, revision E.01, Gaussian, Inc., Wallingford, CT.

(16) Anisimov, V., and Paneth, P. (1999) ISOEFF98. A program for studies of isotope effects using Hessian modifications. *J. Math. Chem. 26*, 75–86.

(17) Schramm, V. L. (1976) Comparison of initial velocity and binding data for allosteric adenosine monophosphate nucleosidase. *J. Biol. Chem. 251*, 3417–3424.

(18) Sievers, A., and Wolfenden, R. (2005) The effective molarity of the substrate phosphoryl group in the transition state for yeast OMP decarboxylase. *Bioorg. Chem. 33*, 45–52.

(19) Morrow, J. R., Amyes, T. L., and Richard, J. P. (2008) Phosphate binding energy and catalysis by small and large molecules. *Acc. Chem. Res. 41*, 539–548.

(20) Tsang, W. Y., Amyes, T. L., and Richard, J. P. (2008) A substrate in pieces: Allosteric activation of glycerol 3-phosphate dehydrogenase (NAD^+) by phosphite dianion. *Biochemistry 47*, 4575–4582.

(21) Go, M. K., Amyes, T. L., and Richard, J. P. (2009) Hydron transfer catalyzed by triosephosphate isomerase. Products of the direct and phosphite-activated isomerization of [1-^{13}C]-glycolaldehyde in D_2O. *Biochemistry 48*, 5769–5778.

(22) Westaway, K. C., Fang, Y. R., MacMillar, S., Mattsson, O., Poirier, R. A., and Islam, S. M. (2008) Determining the transition-state structure for different SN2 reactions using experimental nucleophile carbon and secondary α-deuterium kinetic isotope effects and theory. *J. Phys. Chem. A 112*, 10264–10273.

(23) Thatcher Gregory, R. J. (1993) Anomeric and Associated Stereoelectronic Effects. In *The Anomeric Effect and Associated Stereoelectronic Effects*, pp 6−25, American Chemical Society, Washington, DC.

(24) Carr, C. A., Ellison, S. L. R., and Robinson, M. J. T. (1989) Diverse origins of conformational equilibrium isotope effects for hydrogen in 1,3-dioxans. *Tetrahedron Lett. 30*, 4585–4588.

(25) Forsyth, D. A., and Hanley, J. A. (1987) Conformationally dependent intrinsic and equilibrium isotope effects in N-methylpiperidine. *J. Am. Chem. Soc. 109*, 7930–7932.

(26) Anet, F. A. L., and Kopelevich, M. (1986) Deuterium isotope and anomeric effects in the conformational equilibria of molecules containing CHD-O groups. *J. Am. Chem. Soc. 108*, 2109–2110.

(27) Kirby, A. J. (1987) Mechanism and stereoelectronic effects in the lysozyme reaction. *CRC Crit. Rev. Biochem. 22*, 283–315.

(28) Gonzalez-Segura, L., Witte, J. F., McClard, R. W., and Hurley, T. D. (2007) Ternary complex formation and induced asymmetry in orotate phosphoribosyltransferase. *Biochemistry 46*, 14075–14086.

(29) Henriksen, A., Aghajari, N., Jensen, K. F., and Gajhede, M. (1996) A flexible loop at the dimer interface is a part of the active site of the adjacent monomer of *Escherichia coli* orotate phosphoribosyltransferase. *Biochemistry 35*, 3803–3809.

(30) Scapin, G., Grubmeyer, C., and Sacchettini, J. C. (1994) Crystal structure of orotate phosphoribosyltransferase. *Biochemistry 33*, 1287–1294.

(31) Scapin, G., Ozturk, D. H., Grubmeyer, C., and Sacchettini, J. C. (1995) The crystal structure of the orotate phosphoribosyltransferase complexed with orotate and α-D-5-phosphoribosyl-1-pyrophosphate. *Biochemistry 34*, 10744–10754.

(32) Boehr, D. D., Dyson, H. J., and Wright, P. E. (2006) An NMR perspective on enzyme dynamics. *Chem. Rev. 106*, 3055–3079.

(33) Gao, J., Ma, S., Major, D. T., Nam, K., Pu, J., and Truhlar, D. G. (2006) Mechanisms and free energies of enzymatic reactions. *Chem. Rev. 106*, 3188–3209.

(34) Hammes-Schiffer, S., and Benkovic, S. J. (2006) Relating protein motion to catalysis. *Annu. Rev. Biochem. 75*, 519–541.

(35) Saen-Oon, S., Quaytman-Machleder, S., Schramm, V. L., and Schwartz, S. D. (2008) Atomic detail of chemical transformation at the transition state of an enzymatic reaction. *Proc. Natl. Acad. Sci. U.S.A. 105*, 16543–16548.

(36) Schwartz, S. D., and Schramm, V. L. (2009) Enzymatic transition states and dynamic motion in barrier crossing. *Nat. Chem. Biol. 5*, 551–558.

(37) Sauve, A. A., Cahill, S. M., Zech, S. G., Basso, L. A., Lewandowicz, A., Santos, D. S., Grubmeyer, C., Evans, G. B., Furneaux, R. H., Tyler, P. C., McDermott, A., Girvin, M. E., and Schramm, V. L. (2003) Ionic states of substrates and transition state analogues at the catalytic sites of N-ribosyltransferases. *Biochemistry 42*, 5694–5705.